Supplement of Geosci. Model Dev., 17, 8181–8222, 2024
https://doi.org/10.5194/gmd-17-8181-2024-supplement

Geoscientific Model Development
Open Access
EGU

Supplement of

A dynamical process-based model for quantifying global agricultural ammonia emissions – AMmonia–CLIMate v1.0 (AMCLIM v1.0) – Part 1: Land module for simulating emissions from synthetic fertilizer use

Jize Jiang et al.

Correspondence to: Jize Jiang (jize.jiang@usys.ethz.ch, jize.jiang@ed.ac.uk)

S1 Budgets of TAN and other nitrogen species in soil layers for simulating chemical fertilizer applications

The budget of TAN in each soil layer ($M_{\mathrm{TAN,\,L}}$, g N m^{-2}, given in per unit area; all masses have units of g m^{-2} if not specifically explained) varies as processes can be different. For the top soil layer (0-2 cm), the time-dependent TAN pool is expressed as:

$$\frac{\mathrm{d}M_{\mathrm{TAN,L1}}}{\mathrm{d}t} = I_{\mathrm{TAN}} + F_{\mathrm{TAN}} - F_{\mathrm{NH_3}} - F_{\mathrm{N\ runoff}} - F_{\mathrm{diffusion}} - F_{\mathrm{drainage}} - F_{\mathrm{nitrif}}. \quad \text{(SM1)}$$

For soil layer 2 and 3:

$$\frac{\mathrm{d}M_{\mathrm{TAN,L2,3}}}{\mathrm{d}t} = I_{\mathrm{TAN}} + F_{\mathrm{TAN}} - F_{\mathrm{diffusion}} - F_{\mathrm{drainage\ or\ leaching}} - F_{\mathrm{nitrif}} - F_{\mathrm{uptake}}. \quad \text{(SM2)}$$

The input flux I_{TAN} includes diffusive and drainage fluxes from the layer above for soil layer 2 and 3.

The bottom soil layer acts as a boundary layer of the deeper soils where dissolved nitrogen is lost from the soil column through leaching and diffusion, where the pools and concentrations of nitrogen species are set to 0. The bottom soil layer has a thickness of 14 cm in order to define the transport distance for diffusive fluxes and also to be consistent with the layering of the reanalysis soil data used in the model.

AMCLIM also simulates urea and nitrate in soils. In the top soil layer, the time-dependent urea and nitrate pools are expresses as:

$$\frac{\mathrm{d}M_{\mathrm{urea,L1}}}{\mathrm{d}t} = I_{\mathrm{urea}} - K_{\mathrm{Urea}}M_{\mathrm{Urea}} - F_{\mathrm{urea\ runoff}} - F_{\mathrm{diffusion}} - F_{\mathrm{drainage}}, \quad \text{(SM3)}$$

$$\frac{\mathrm{d}M_{\mathrm{nitrate,L1}}}{\mathrm{d}t} = F_{\mathrm{nitrif}} - F_{\mathrm{nitrate\ runoff}} - F_{\mathrm{diffusion}} - F_{\mathrm{drainage}}. \quad \text{(SM4)}$$

For soil layer 2 and 3:

$$\frac{\mathrm{d}M_{\mathrm{urea,L2,3}}}{\mathrm{d}t} = I_{\mathrm{urea}} - K_{\mathrm{Urea}}M_{\mathrm{Urea}} - F_{\mathrm{diffusion}} - F_{\mathrm{drainage}}, \quad \text{(SM5)}$$

$$\frac{\mathrm{d}M_{\mathrm{nitrate,L2,3}}}{\mathrm{d}t} = F_{\mathrm{nitrif}} - F_{\mathrm{diffusion}} - F_{\mathrm{drainage}} - F_{\mathrm{uptake}}. \quad \text{(SM6)}$$

The fluxes have been explained in Sections 2.2.1 (I_{TAN} – direct input of TAN species, such as ammonium or ammonia; I_{TAN} – direct input of urea from fertilizer; F_{TAN} – TAN production through urea or UA hydrolysis and decomposition of organic N; $F_{\mathrm{NH_3}}$ – flux of NH_3 volatilization; $F_{\mathrm{TAN/urea/nitrate\ runoff}}$ – flux of surface TAN, urea or nitrate runoff; $F_{\mathrm{diffusion}}$ – diffusive fluxes; F_{drainage} – flux of drainage; F_{leaching} – flux of leaching; F_{nitrif} – nitrification; F_{uptake} – flux of N uptake by plants/crops; all N fluxes/flows have units of g N m^{-2} s^{-1} if not specifically explained).

Urea hydrolysis is one of the main inputs to soil TAN pool. The hydrolysis of urea is dependent on environmental factors, such as temperature and water content of the soil. The hydrolysis rate of urea (K_{Urea}, s^{-1}) is parameterized as follows by assuming a first order reaction according to Sherlock and Goh (1984):

$$\frac{\mathrm{d}M_{\mathrm{Urea}}}{\mathrm{d}t} = -K_{\mathrm{Urea}}M_{\mathrm{Urea}}, \quad \text{(S7)}$$

$$K_{\mathrm{Urea}} = 1 - \exp\left(-k_h \cdot WFPS \cdot A_h\right), \quad \text{(S8)}$$

$$A_h = 0.25 \exp(0.0693\,(T - 273.15)), \quad \text{(S9)}$$

where k_h is the urea hydrolysis constant for urine (6.4×10^{-5} s^{-1} or 0.23 h^{-1}; Sherlock and Goh (1984)) and for urea in soils (8.3×10^{-6} s^{-1} or 0.03 h^{-1}; Dutta et al. (2016)). *WFPS* is the water-filled pore space. A_h is a temperature correction dependence, and T is the temperature in Kelvin (K).

S2 Adsorption coefficient of NH_4^+ on solid particles

Soils can adsorb NH_4^+ due to cation exchange, and the adsorption of NH_4^+ on soil solids varies between different soils (Buss et al., 2004). The cation exchange capacity of soils is difficult to simulate especially on a global scale. Therefore, the partitioning coefficient K_d (m^3 m^{-3}) used to determine the NH_4^+ adsorption is derived from an empirical relationship depending on the fractional soil clay content (f_{clay}) to which the soil cation exchange capacity is related (Dutta et al., 2016). The equation is expressed as:

$$K_d = 0.5\left(7.2733 {f_{clay}}^3 - 11.22 {f_{clay}}^2\right) + 5.7198 f_{clay} + 0.0263. \quad \text{(SM10)}$$

S3 Nitrification process

Nitrification is considered to take place in soils and solid manure systems exposed to oxygen. In contrast, for liquid systems, such as slurry system or lagoon, nitrification is considered to be absent or negligible due to the high water content that reduces oxygen availability.

A first-order reaction is used to determine nitrification as shown in Eq. (12). The optimum nitrification rate ($K_{nitrif,opt}$) is set to be 10 % per day, and the nitrification rate K_{nitrif} is affected by temperature, water content, and pH as shown in Eq. (12) (Parton et al., 1996, 2001). The dependence of each factor is expressed by the following equations. The temperature dependence is taken from Stange and Neue (2009):

$$K_{\text{nitirif,T}} = \left(\frac{T_{\max,\text{nitrif}} - T_{\text{gnd}}}{T_{\max,\text{nitrif}} - T_{\text{opt,nitrif}}}\right)^{a_\Sigma} \exp\left(a_\Sigma\left(\left(\frac{T_{\max,\text{nitrif}} - T_{\text{gnd}}}{T_{\max,\text{nitrif}} - T_{\text{opt,nitrif}}}\right)\right)\right), \quad \text{(SM11)}$$

where T_{gnd} is the ground temperature. The maximum temperature ($T_{max,nitrif}$) and optimum temperature ($T_{opt,nitrif}$) for microbial activity is 313 K and 301 K, respectively. a_Σ is an empirical factor that equals to 2.4 for manure; optimum temperature is 303 K and a_Σ is 1.8 for synthetic fertilizer (Stange and Neue, 2009).

The water content and pH dependence are taken from the empirical function of Patron et al. (1996)

$$k_{\text{nitrif,WFPS}} = \left(\frac{WFPS - b}{a - b}\right)^{d\cdot\left(\frac{b-a}{a-c}\right)} \left(\frac{WFPS - c}{a - c}\right)^{d}, \quad \text{(SM12)}$$

where *WFPS* is the water-filled porosity of soil and is set to 1.0 for solid manure storage. Coefficients a, b, c and d are equal to 0.60, 1.27, 0.0012 and 2.84, respectively (Parton et al., 1996).

$$k_{\text{nitrif,pH}} = 0.56 + \frac{\tan^{-1}(0.45\pi(\text{pH} - 5))}{\pi}. \quad \text{(SM13)}$$

Nitrification is mainly found to take place in soils at pH ranging between 5.5 to 10, with the optimum pH at around 8.5, and the process mainly ceases in soils under natural pH less than 5.0 (Parton et al., 1996). In AMCLIM-Land, the pH dependence for nitrification rate is a trigonometric function from Parton et al. (1996).

S4 Nitrogen and water uptake by crops

Nitrogen uptake by plants in AMCLIM-Land is assumed to take place in soil layers 2 and 3, which can be calculated by Eq. (13) in Sect.2.2.1. Uptake is not treated in the top soil layer (layer 1), which focuses on the ammonia–atmosphere exchange interface (Sect.2.2.1). AMCLIM–Land uses a root uptake scheme derived from several studies (Riedo et al., 1998; Thornley, 1991; Thornley and Cannell, 1992; Thornley and Verberne, 1989). Crops can take up both ammonium and nitrate from the soils, together termed as M_{Neff}, as expressed by the follows:

$$M_{\mathrm{Neff}} = M_{\mathrm{NH_4^+}} + a_{\mathrm{plant}} M_{\mathrm{NO_3^-}}, \quad \text{(SM14)}$$

where $M_{\mathrm{NH_4^+}}$ and $M_{\mathrm{NO_3^-}}$ are ammonium and nitrate pools in soils. A dimensionless parameter a_{plant} varies between 0.5 to 1.0 depending upon temperature, and is calculated by the following equation:

$$a_{\mathrm{plant}} = a_{20} - (a_{20} - a_{10}) \frac{(20 - T_{\mathrm{gnd}})}{(20 - 10)}, \quad \text{(SM15)}$$

where a_{20} and a_{10} are reference values at 20 and 10 °C, respectively (Thornley and Verberne, 1989). However, this equation is only applicable between 10 and 20 °C so is extrapolated to a broader temperature range as the following equation:

$$a_{\mathrm{plant}} = 0.25 e^{0.0693 T_{\mathrm{gnd}}}. \quad \text{(SM16)}$$

The integrated root activity parameter α_{root} is determined by the following equation:

$$\alpha_{\mathrm{root}} = \sigma_{\mathrm{N}} \sum_{i=1}^{4} v_i W_{r,i}, \quad \text{(SM17)}$$

where $W_{\mathrm{r,i}}$ (g m^{-2}) is root structural dry matter and v_{i} is the corresponding root activity weighting parameter (Thornley and Verberne, 1989). There are four components in $W_{\mathrm{r,i}}$ that represent the structural dry matter of roots at different stages (i.e., four age categories of roots from young to mature). The values of $W_{\mathrm{r,i}}$ were taken from Thornley et al (1991), which are equivalent to 20, 40, 60, 80 g m^{-2}. Mature roots have larger $W_{\mathrm{r,i}}$ values. The root activity weighting parameter v_{i} changes as plants grow, i.e., larger values refer to more mature roots of the plant. AMCLIM-Land uses a set of empirical values to represent v_{i}, which describes the status of roots at six growing stages (Table A1). The six growing stages are evenly distributed during the growing season of a crop.

Table S1. Root activity weighting parameters at different crop growing stage.

	Stage 1	Stage 2	Stage 3	Stage 4	Stage 5	Stage 6
v_1	0.1	1.0	1.0	0.5	0.25	0.1

v_2	0.1	0.5	1.0	1.0	0.5	0.25
v_3	0.1	0.25	0.5	1.0	1.0	1.0
v_4	0.1	0.1	0.25	0.5	1.0	1.0

σ_N (g N g^{-1} d^{-1}) is the temperature-dependent root activity parameter for nitrogen, which is calculated by the following equation:

$$\sigma_N = \sigma_{20} f_T, \quad \text{(SM18)}$$

where σ_{20} is a reference value that is set at 0.05 at 20 °C (Thornley and Verberne, 1989), and the temperature dependence (f_T) is identical as Eq. (SM16).

The combined response factor $J_{C,N}$ (dimensionless) for plant uptake to substrate carbon and nitrogen from the soil is calculated by the following equation:

$$J_{C,N} = 1 + \frac{K_{CUN}}{C}\left(1 + \frac{N}{J_{NUN}}\right), \quad \text{(SM19)}$$

where K_{CUN} (0.05[C]) and J_{NUN} (0.005[N]) are constants. In this equation, C (g C m^{-2}) and N (g N m^{-2}) are substrate concentration of carbon and nitrogen (Riedo et al., 1998; Thornley, 1991; Thornley and Cannell, 1992; Thornley and Verberne, 1989), respectively. As the model does not simulate plant dynamics, C and N are represented by fixed values of 40 g C m^{-2} and 4 g N m^{-2}, respectively (Riedo et al., 1998).

Combining these terms, plant uptake of N (F_{uptake}) can be expressed as (Riedo et al., 1998; Thornley, 1991; Thornley and Cannell, 1992):

$$F_{uptake} = \frac{\alpha_{root}}{J_{C,N}} \frac{M_{Neff}}{M_{Neff} + K_{Neff}} = \sigma_N \sum_{i=1}^{4} v_i W_{r,i} \frac{M_{NH_4^+} + a_{plant,nit} M_{NO_3^-}}{M_{NH_4^+} + a_{plant,nit} M_{NO_3^-} + K_{Neff}} \frac{1}{1 + \frac{K_C}{C}\left(1 + \frac{N}{K_N}\right)}. \quad \text{(SM20)}$$

where K_{Neff} is a root activity parameter, set at a constant of 5 g N m^{-2} (Riedo et al., 1998). Water uptake (W_{uptake}, m s^{-1}) by crops is represented by a simple empirical equation that is related to the soil water content (Dardanelli et al., 2004), which is expressed as follows:

$$W_{uptake} = K_{uptake}(\theta - \theta_{wp}), \quad \text{(SM21)}$$

where K_{uptake} is an empirical coefficient that equals to 1.1×10^{-6} s^{-1} (0.096 d^{-1}) (Dardanelli et al., 2004).

S5 Calculation of soil resistances

Aqueous and gaseous diffusion of nitrogen species in soils are constrained by soil resistances. The soil resistance is determined by the following equation:

$$R_{soil,aq/gas} = \frac{\Delta z_{soil}}{\xi_{aq/gas}(\theta) D^{aq/gas}_{NH_4/NH_3}}, \quad \text{(SM22)}$$

where Δz_{soil} (m) is the transport distance in soils, which is treated as the distance between the mid-points of each soil layer. The molecular diffusivity ($D^{\mathrm{aq/gas}}_{\mathrm{NH_4/NH_3}}$, $\mathrm{m^2\ s^{-1}}$) is multiplied by a soil tortuosity factor, $\xi_{\mathrm{aq/gas}}(\theta)$, to adjust for the soil water content as well as the porosity (Millington and Quirk, 1961; Móring et al., 2016; Vira et al., 2020). The molecular diffusivity and tortuosity factor are calculated by the following equations:

$$D^{\mathrm{aq/gas}}_{\mathrm{NH_4/NH_3}} = \begin{cases} 9.8\times10^{-10}\cdot 1.03^{T-273.15}, & \text{for } \mathrm{NH_4^+} \\ \frac{10^{-7}\cdot T^{1.75}(1/m_{\mathrm{air}}+1/m_{\mathrm{NH_3}})^{0.5}}{p[(\sum_{\mathrm{air}} v_i)^{1/3}+(\sum_{\mathrm{NH_3}} v_i)^{1/3}]^2}, & \text{for } \mathrm{NH_3} \end{cases}, \quad \text{(SM23)}$$

where m_{air} and $m_{\mathrm{NH_3}}$ are molecular weight of air and NH_3, respectively, using values of 29 g mol^{-1} and 17 g mol^{-1}. $\sum_{\mathrm{air}} v_i$ (20.1) and $\sum_{\mathrm{NH_3}} v_i$ (14.9) are the atomic diffusion volumes for air and NH_3 (Perry and Green, 2008), and p (Pa) is pressure in the atmosphere.

$$\xi_{\mathrm{aq/gas}}(\theta) = \begin{cases} \frac{(\theta-\theta_{\mathrm{sat}})^{\frac{8.5}{3}}}{\theta_{\mathrm{sat}}^{1.7}}, & \text{for gaseous diffusion} \\ \frac{\theta^{\frac{8.5}{3}}}{\theta_{\mathrm{sat}}^{1.7}}, & \text{for aqueous diffusion} \end{cases}, \quad \text{(SM24)}$$

where θ_{sat} is soil water content at saturation. The tortuosity factors are calibrated by site simulations using AMCLIM under the conditions of the GRAMINAE field experiment (see Sect.2.3.1).

S6 Concentrations of nitrogen species at surface

Volatilization and runoff take place at the land surface, with these fluxes being primarily driven by nitrogen concentrations at the surface. To take into account the soil resistance and heterogeneity of the soil, the surface concentrations of nitrogen species are not calculated from dividing the mass of nitrogen in the soil layer by the volume (or the thickness over unit areas), but are solved by assuming that the upward diffusion (from the mid-point of the top soil layer to the surface) is equal to the volatilization and runoff, as expressed by Eq. (14). Therefore, Eq. (14) can be expanded as:

$$\frac{[\mathrm{NH_3(g)}]_{\mathrm{srf}}-\chi_{\mathrm{atm}}}{R_{\mathrm{atm}}} + q_r\cdot[\mathrm{TAN(aq)}]_{\mathrm{srf}} = \frac{[\mathrm{TAN(aq)}]_{\mathrm{L1}}-[\mathrm{TAN(aq)}]_{\mathrm{srf}}}{R_{\mathrm{L1,aq}}} + \frac{[\mathrm{NH_3(g)}]_{\mathrm{L1}}-[\mathrm{NH_3(g)}]_{\mathrm{srf}}}{R_{\mathrm{L1,gas}}}. \quad \text{(SM25)}$$

The aqueous concentration of TAN at the surface can be solved as:

$$[\mathrm{TAN(aq)}]_{\mathrm{srf}} = \frac{[\mathrm{TAN(aq)}]_{\mathrm{L1}}\cdot\left(\frac{1}{R_{\mathrm{L1,aq}}}+\frac{K_{\mathrm{NH_3}}}{R_{\mathrm{L1,gas}}}\right)+\frac{\chi_{\mathrm{atm}}}{R_{\mathrm{atm}}}}{q_{\mathrm{r}}+\frac{1}{R_{\mathrm{L1,aq}}}+K_{\mathrm{NH_3}}\cdot\left(\frac{1}{R_{\mathrm{L1,gas}}}+\frac{1}{R_{\mathrm{atm}}}\right)}, \quad \text{(SM26)}$$

and gaseous NH_3 concentration at the surface can be solved subsequently (combined with Eq. (6)).

S7 Water drainage and percolation flux

Leaching of nitrogen from soils is determined by multiplying the aqueous concentrations of each species by the percolation flux of water. The percolation flux of water is the minimum value between the soil hydraulic conductivity and the drainage potential as shown in Eq. (17).

The soil hydraulic conductivity (K_s) is related to the soil water content and the soil characteristics, which is approximated by the following equation (Li et al., 2019):

$$K_{\mathrm{s}} = \frac{\theta}{\theta_{\mathrm{sat}}} K_{\mathrm{sat}}, \quad \text{(SM27)}$$

Where $K_{\mathrm{sat}} = 2.2 \times 10^{-7} e^{x}$, (SM28)

given $x = 7.755 + 0.0352 f_{\mathrm{silt}} - 0.967 BD_{\mathrm{soil}}{}^{2} - 0.000484 f_{\mathrm{clay}}{}^{2} - 0.000322 f_{\mathrm{silt}}{}^{2} + \frac{0.001}{f_{\mathrm{silt}}} - \frac{0.748}{f_{\mathrm{som}}} - 0.643 \log_e f_{\mathrm{silt}} - 0.01398 BD_{\mathrm{soil}} \cdot f_{\mathrm{silt}} - 0.1673 BD_{\mathrm{soil}} \cdot f_{\mathrm{som}}$, (SM29)

and where K_{sat} (m s^{-1}) is the soil hydraulic conductivity at saturation, which is dependent on the fractional soil silt (f_{silt}) and clay content (f_{clay}), bulk density of soil (BD_{soil}, g cm^{-3}) and fractional soil organic matter content (f_{som}). The information of soil properties is from the Regridded Harmonized World Soil Database (HWSD) v1.2 (FAO and IIASA, 2012; Wieder et al., 2014).

The drainage potential of a soil layer is calculated by the following equation:

$$D_{\mathrm{pot}} = \max\left(0, \frac{\theta - \theta_{\mathrm{fc}}}{z t_{\mathrm{fc}}}\right), \quad \text{(SM30)}$$

where t_{fc} is a reference time that soil water content reaches field capacity, which is set at 24 h. The field capacity of soil is determined from the bulk density (BD) (Li et al., 2019), as expressed by the following equation:

$$\theta_{\mathrm{fc}} = 0.45 - 0.06 BD_{\mathrm{soil}}{}^{2}. \quad \text{(SM31)}$$

S8 Fertilizer types from IFA and disaggregation of total nitrogen rates

AMCLIM-Land uses nitrogen chemical fertilizer consumption statistics at country-level from the International Fertilizer Association (IFA, 2023). Nitrogen fertilizer types provide in the IFA dataset includes direct NH_3, ammonium phosphate (AP), ammonium sulphate (AS), ammonium nitrate (AN), calcium ammonium nitrate (CAN), NK compound fertilizer (NK), NPK compound fertilizer (NPK), nitrogen solution, other NP fertilizer (other NP), urea, and other N straight fertilizer. It is assumed that NK compound fertilizer, NPK compound fertilizer and other NP fertilizer have the same amount of ammonium and nitrate on an equivalent basis. Nitrogen solution is assumed to contain 75 % of ammonium and 25 % nitrate (Vira et al., 2020). Other N straight fertilizer is treated as urea in AMCLIM-Land. The nitrogen in ammonium fertilizer, urea fertilizer and nitrate fertilizer can be calculated accordingly by the following equations:

$$Amm_{\mathrm{N}} = NH_3 + AP_{\mathrm{N}} + AS_{\mathrm{N}} + 0.5(AN_{\mathrm{N}} + CAN_{\mathrm{N}} + NK + NPK + other\ NP) + 0.75 Nsolution, \quad \text{(SM32)}$$

$$Urea_{\mathrm{N}} = Urea + Other\ N\ straight, \quad \text{(SM33)}$$

$$Nit_{\mathrm{N}} = 0.5(AN_{\mathrm{N}} + CAN_{\mathrm{N}} + NK + NPK + other\ NP) + 0.25Nsolution. \quad \text{(SM34)}$$

The fraction of the major three nitrogen fertilizer groups (ammonium, urea and nitrate) is then calculated as follows:

$$f_{\mathrm{fert(j)}} = \frac{M_{\mathrm{fert(j)}}}{\sum_{\mathrm{j=1}}^{3} M_{\mathrm{fert(j)}}}. \quad \text{(SM35)}$$

The nitrogen application and fraction of three types of fertilizers as derived here for 2010 and 2018 are shown in Figure S1 and S2.

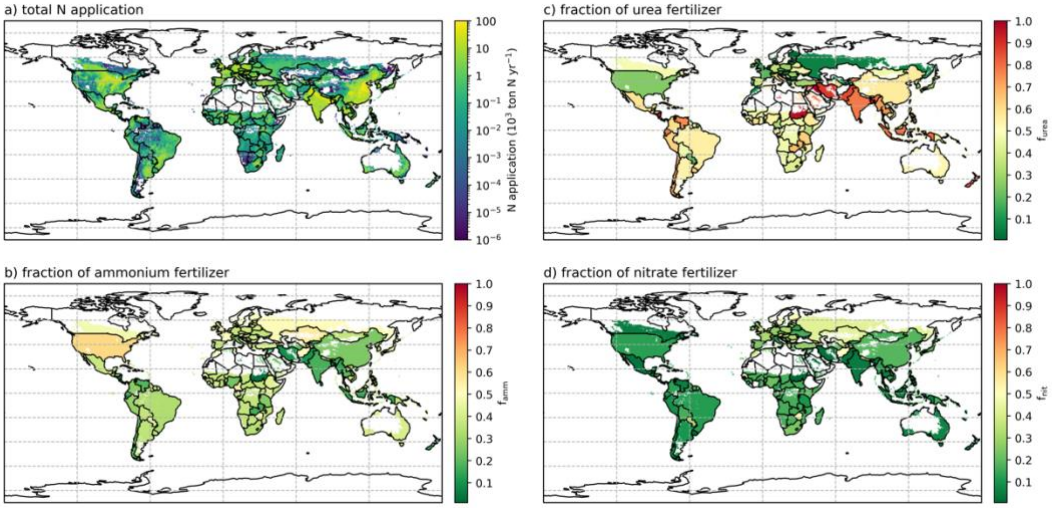

Figure S1. Fertilizer information of 2010. (a) Total nitrogen application rate. (b) Fraction of ammonium fertilizer. (c) Fraction of urea fertilizer. (d) Fraction of nitrate fertilizer.

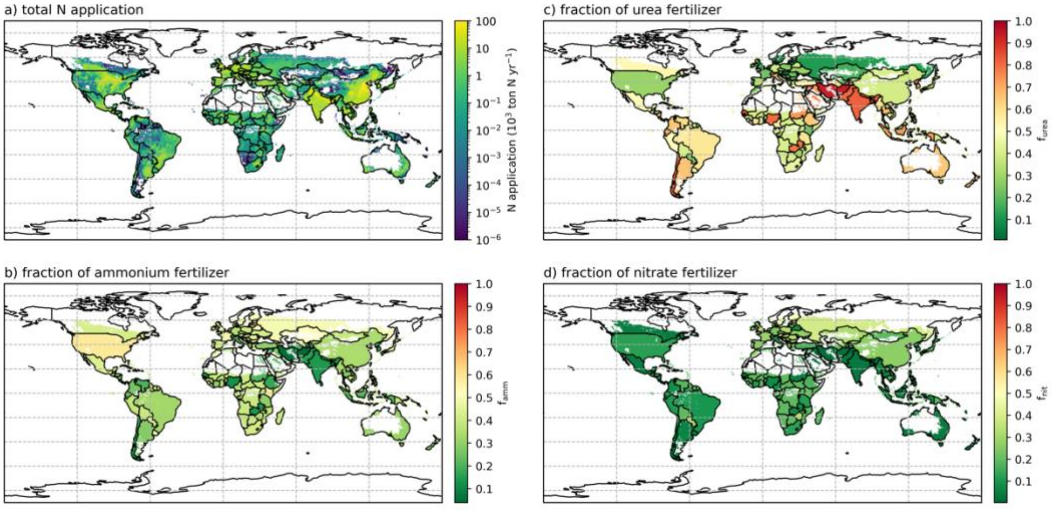

Figure S2. Same as Fig. S1, but for 2018.

S9 Model diagnostic for the GRAMINAE site simulations

Figure S3 shows the modelled concentrations of N species in soils, as well as soil resistances and the NH_3 emissions. Figure S3 includes aqueous TAN and gaseous NH_3; in this paragraph, TAN refers only to aqueous TAN only excluding solid exchangeable TAN.

The simulated concentrations of surface gaseous NH_3 are found to be much higher than the atmospheric NH_3 concentration at 1 m. Surface NH_3 concentrations range between 100 and 150 μg m^{-3} on the first day, and between 50 to 100 μg m^{-3} for the rest of the week, while the atmospheric concentrations of NH_3 are mostly within the range between 0 to 25 μg m^{-3}. Two evident peaks in surface NH_3 concentrations that are larger than 200 μg m^{-3} on 10 June can be seen. In contrast to the surface gaseous NH_3 concentrations, surface TAN concentration shows greater variation within a day, and its trends are opposite to the emissions, with higher values at night and lower values in the day. In the top soil layer (0–2 cm), TAN concentrations show a smooth declining curve from 1750 g m^{-3} to less than 250 g m^{-3} throughout the simulated period (Fig.S3c), indicating depletion of the TAN pool due to N losses through multiple pathways, which together act as a 1st order loss process. The simulated gaseous NH_3 concentrations of this soil layer show large variations due to the diurnal cycle in the temperature.

Soil resistances that constrain aqueous diffusion are found to be much larger than the resistance for gaseous diffusion of NH_3 (Fig.S3c). It is found that soil resistances are larger at night than day time due to low temperature, which slows down diffusion fluxes through the soil. When there are no runoff fluxes (i.e., no precipitation), upward soil diffusion fluxes are only balanced by the volatilization. As a solved variable by assuming an equilibrium state, surface TAN concentrations therefore tend to be high at night, leading to low concentration gradients. Meanwhile, since the resistances are large, upwards diffusive fluxes become smaller, which limits the surface fluxes (i.e., volatilization).

An averaged value of measured soil pH of ~6.3 was used for the simulations (Fig.S3d) based on field measurements at the site (Sutton et al., 2009a; Sutton et al., 2009b). As a result, the gamma value ($([NH_4^+]/[H^+]$) of the top soil layer derived from the TAN concentration is shown as a smooth decaying curve. The modelled gamma values of the top soil layer were between 50000 and 25000, which are the same order of magnitude as the estimated measured values (exact measured values of gamma are not available; crude values are estimated from Fig.3 in Personne et al. (2009); Sutton et al. (2009b) by vision) and are comparable with the simulated gamma of the litter layer by Personne et al. (2009). Surface runoff was directly represented by the precipitation, and the modelled NH_3 emissions show sharp declines immediately after rain (e.g., 5 June evening) because the surface runoff is a competing pathway to the volatilization, which together deplete the TAN pool of the soil (Fig.3). The GRAMINAE measurements focused on NH_3 fluxes and did not include quantification of surface run-off, preventing site validation of this term. For example, the drivers for run off and leaching are similar, and would both lead to loss of ammonium (thereby reducing NH_3 emissions), especially for the soil in question with low cation exchange capacity site (Sutton et al., 2009a; Sutton et al., 2009b). For the entire simulated period of 5 to 15 June, AMCLIM-Land estimated

that 10.4 % of the applied ammonium N is estimated to be lost due to NH_3 emissions to the air, 1.1 % is washed off by rainfall (runoff), 13.4 % is converted to NO_3^- through nitrification, and the remaining 75.1 % of N is retained in the soil.

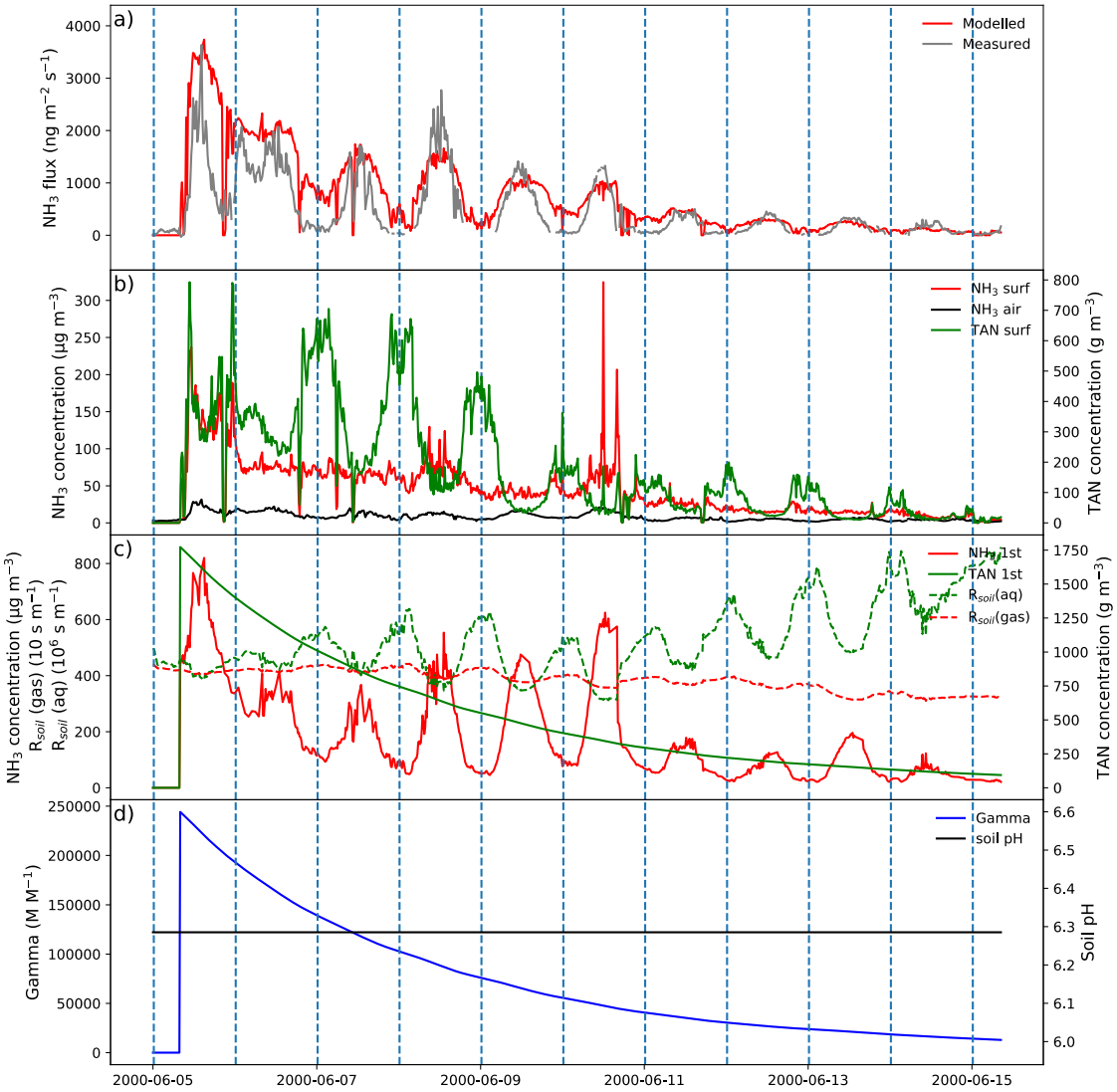

Figure S3. Modelled variables in the site simulations for NH_3 emissions from a post-cutting grassland after fertilization in Braunschweig, Germany, from 5 June 2000 to 15 June 2000 (Sutton et al., 2009a; Sutton et al., 2009b) by AMCLIM–Land. (a) Modelled and measured NH_3 emissions. (b) Solved concentrations of TAN and NH_3 at the surface and the atmospheric concentration of NH_3. (c) Concentrations of TAN and NH_3 of the 1st (top) soil layer, and soil resistances for aqueous and gaseous diffusions. (d) Gamma value ($[NH_4^+]/[H^+]$) of the 1st (top) soil layer (0.3-2 cm depth) and soil pH used in AMCLIM–Land.

S10 Sensitivity test of temporal resolutions of AMCLIM

Model performance at various temporal resolutions, including time-steps at 1 min, 15 mins, 1 hour, 3 hours, 6 hours, 12 hours and 24 hours (as shown by Fig. S4). By decreasing the temporal resolution from 15 mins to 6 hours, the model was still able to capture the main temporal variations in fluxes and to reproduce the peak emissions of each day, while giving a reasonable estimate of cumulative NH_3 emissions. However, when the temporal resolution decreased to 8 hours and even less, the model started to underestimate NH_3 emissions and was not capable of reproducing the emission peaks. The GRAMINAE campaign has shown that the sub-hourly variations in NH_3 fluxes have been well captured by the measurements. Meanwhile, the meteorological inputs that drive the AMCLIM model have a temporal resolution of 15 mins. By simply increasing the temporal resolution of simulations (reduce the time-step) without higher resolution input, the model results are insignificantly different, but the computational costs will increase enormously (running the model at 1 min time-step but use the same meteorology for a 15 mins window leads to only a 4.1% difference, which does not justify the substantial increase in computational costs). Therefore, global simulations were performed at an hourly time step.

Both measurement and model demonstrate that diurnal variability is a predominant feature of NH_3 emissions. To what extent a model can reproduce the temporal variations in NH_3 fluxes should be an important factor in model evaluation. Models that provide comparable cumulative NH_3 emissions relative to measurements can be further improved to address their capability of capturing temporal variations in the NH_3 emission at daily or sub-daily scale.

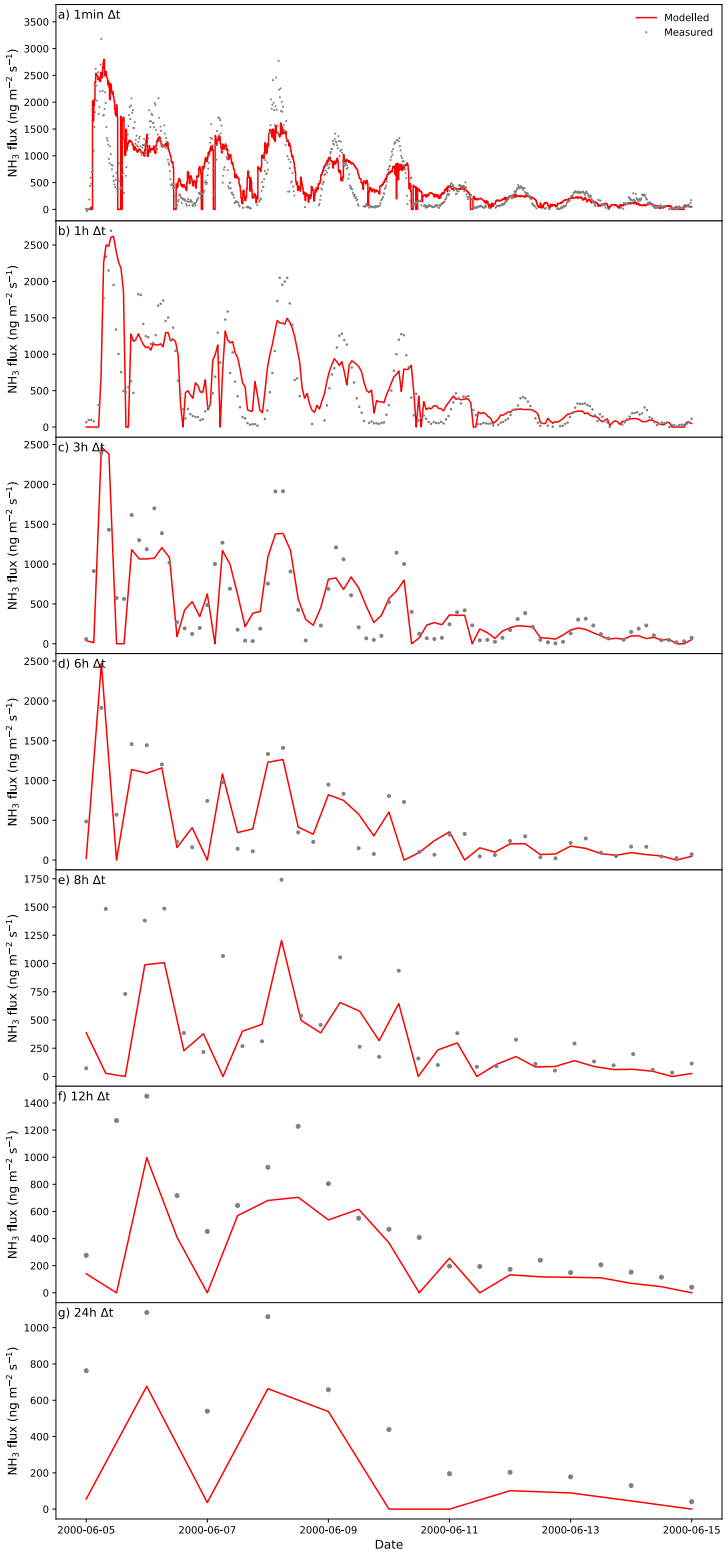
a) 1min Δt
b) 1h Δt
c) 3h Δt
d) 6h Δt
e) 8h Δt
f) 12h Δt
g) 24h Δt
Modelled
Measured
NH3 flux (ng m−2 s−1)
Date
2000-06-05
2000-06-07
2000-06-09
2000-06-11
2000-06-13
2000-06-15

Figure S4. Comparisons between measured and modelled NH_3 emissions with modelling time-steps varied from 1min to 24h. Simulated cumulative NH_3 fluxes were 0.51 g m^{-2} for 1min time-step, 0.36 g m^{-2} for 3h time-step, 0.34 g m^{-2} for 6h time-step, 0.25 g m^{-2} for 8h time-step, 0.24 g m^{-2} for 12h time-step and 0.18 g m^{-2} for 24h time-step. These values compare with the measured cumulative fluxes of 0.32±0.07 g m^{-2}.

S11 Model symbols

a_{plant}	dimensionless parameter for plant activity	
a_{Σ}	empirical factor for nitrification process	1.8 (synthetic fertilizer)
A_h	temperature correction dependence for urea hydrolysis	
BD_{soil}	bulk density of soil	g cm^{-3}
C	substrate concentration of carbon	g C m^{-2}
$D^{aq/gas}_{NH_4/NH_3}$	molecular diffusivity	m^2 s^{-1}
D_{pot}	water drainage potential	m s^{-1}
f_{clay}	fractional soil clay content	
f_{fert}	fraction of fertilizer type used	
f_{silt}	fractional silt content of soil	
f_{som}	fractional soil organic matter content	
f_{tech}	fraction of application technique used	
f_T	temperature dependence of root activity	
$F_{diffusion\ to\ surface}$	upward diffusive fluxes to surface	g N m^{-2} s^{-1}
$F_{diffusion(aq/gas)}$	diffusive fluxes	g N m^{-2} s^{-1}
$F_{drainge}$	flux of N drainage	g N m^{-2} s^{-1}
$F_{leaching}$	flux of leaching	g N m^{-2} s^{-1}
F_{L_N}	sum of losses of N compound	g N m^{-2} s^{-1}
F_{NH_3}	flux of NH_3	g N m^{-2} s^{-1}
$F_{N\ runoff}$	flux of surface N runoff	g N m^{-2} s^{-1}
$F_{N,activity}$	annual total nitrogen from agricultural activity	g N m^{-2} yr^{-1}
$F_{nitrate\ runoff}$	flux of surface nitrate runoff	g N m^{-2} s^{-1}
F_{nitrif}	flux of nitrification	g N m^{-2} s^{-1}
F_{P_N}	sum of production (including inputs) of N compound	g N m^{-2} s^{-1}
$F_{rainfall}$	rainfall	mm s^{-1}
F_{TAN}	production of TAN	g N m^{-2} s^{-1}
$F_{TAN\ runoff}$	flux of surface TAN runoff	g N m^{-2} s^{-1}
F_{uptake}	flux of N uptake by plants/crops	g N m^{-2} s^{-1}

$F_{\text{urea runoff}}$	flux of surface urea runoff	g N m^{-2} s^{-1}
I_{TAN}	direct input of TAN species	g N m^{-2} s^{-1}
$J_{\text{C,N}}$	combined response factor for substrate C and N level	
k	von Karman constant	0.41
k_{G}	gaseous transfer coefficient for NH_3	m s^{-1}
k_{h}	urea hydrolysis constant	s^{-1}
k_{L}	aqueous transfer coefficient for TAN	m s^{-1}
$k_{\text{nitrif,pH}}$	pH dependence of nitrification rate	
$k_{\text{nitrif,T}}$	temperature dependence of nitrification rate	
$k_{\text{nitrif,WFPS}}$	water-filled pore space dependence of nitrification rate	
K_{d}	partition coefficient of soil adsorbed of TAN	m^3 m^{-3}
K_{N}	conversion rate at which a N compound decomposes to form TAN	s^{-1}
K_{Neff}	correction constant for root activity	g N m^{-2}
K_{NH_3}	combined coefficient of Henry and dissociation equilibria	
K_{nitrif}	rate of nitrification	s^{-1}
$K_{\text{nitrif,opt}}$	optimum nitrification rate	0.1 d^{-1}
K_{s}	soil hydraulic conductivity	m s^{-1}
K_{sat}	soil hydraulic conductivity at saturation	m s^{-1}
K_{uptake}	plant water uptake coefficient	0.096 d^{-1}
K_{Urea}	rate of urea hydrolysis	s^{-1}
m_{air}	molecular weight of air	29 g mol^{-1}
m_{NH_3}	molecular weight of NH_3	17 g mol^{-1}
$M_{\text{H}_2\text{O}}$	mass of water	g m^{-2}
M_{N}	mass of N species	g N m^{-2}
M_{Neff}	mass of effective available N for the plant	g N m^{-2}
M_{nitrat}	mass of nitrate	g N m^{-2}
$M_{\text{NH}_3,\text{g}}$	mass of gas NH_3	g N m^{-2}
$M_{\text{NH}_4^+}$	mass of NH_4^+	g N m^{-2}
$M_{\text{NH}_4^+}$	mass of exchangeable solid NH_4^+ (adsorbed NH_4^+)	g N m^{-2}
M_{TAN}	mass of TAN in all phases	g N m^{-2}
$M_{\text{TAN,aq}}$	mass of aqueous TAN	g N m^{-2}

M_{Urea}	mass of urea	g N m^{-2}
N	substrate concentration of nitrogen	g N m^{-2}
p	atmospheric pressure	Pa
P_{V}	percentage of N volatilizes as NH_3	%
q_{p}	subsurface percolation flux of water	m s^{-1}
q_{r}	surface runoff flux of water	m s^{-1}
Q_{in}	airflow rate of animal house	m^3 s^{-1}
R	resistance constraining fluxes	s m^{-1}
R_{a}	aerodynamic resistance	s m^{-1}
$R_{\mathrm{aq/gas}}$	resistance that constrains the aqueous or gaseous diffusion processes	s m^{-1}
R_{atm}	atmospheric resistances	s m^{-1}
R_{b}	boundary layer resistance	s m^{-1}
RH	relative humidity	%
t_{fc}	reference time for soil water content reaching field capacity	24 h
$T_{\mathrm{max,nitrif}}$	maximum temperature for microbial activity for nitrification	313 K
$T_{\mathrm{opt,nitrif}}$	optimum temperature for microbial activity for nitrification	301 K
T	temperature	K or °C
T_{gnd}	ground temperature	°C
u	wind speed at reference height z	m s^{-1}
u_*	friction velocity	m s^{-1}
v	kinematic viscosity	m^2 s^{-1}
v_{i}	root activity weighting parameter	
$V_{\mathrm{H_2O}}$	volume of water	mL m^{-2}
$WFPS$	water-filled pore space	
w_{irr}	irrigation	m
$W_{\mathrm{r,i}}$	root structural dry matter components	g m^{-2}
W_{uptake}	water uptake by crops	m s^{-1}
z_0	roughness length	m
z_{i}	thickness of soil layer i	m

α_{root}	integrated root activity parameter for N uptake	g N m^{-2} s^{-1}
Γ	emission potential ($[NH_4^+]/[H^+]$)	
σ_{20}	reference root activity parameter at 20 °C	0.05 (20 °C)
σ_{N}	temperature-dependent root activity parameter	g N g^{-1} d^{-1}
ε	porosity of soil	m^3 m^{-3} or m m^{-1}
θ	soil volumetric water content	m^3 m^{-3} or m m^{-1}
θ_{fc}	field capacity	m^3 m^{-3} or m m^{-1}
θ_{irr}	soil water content of irrigated croplands	m^3 m^{-3} or m m^{-1}
θ_{manure}	volumetric water content of manure	m^3 m^{-3} or m m^{-1}
θ_{rea}	reanalysis soil water content	m^3 m^{-3} or m m^{-1}
θ_{sat}	soil water content at saturation	m^3 m^{-3} or m m^{-1}
θ_{wp}	soil wilting point	m^3 m^{-3} or m m^{-1}
$\xi_{\mathrm{aq/gas}}(\theta)$	tortuosity factors	
ρ_{air}	air density	kg m^{-3}
ρ_{water}	density of water	kg m^{-3}
χ	concentration of gas NH_3	g m^{-3}
χ_{atm}	concentration of atmospheric NH_3	g m^{-3}
$\chi(\mathrm{z})$	concentration of gas NH_3 at height z	g m^{-3}
[N]	concentration of N species	g mL^{-1}
[N(sfc)]	surface concentration of N species	g mL^{-1}
[N(soil)]	concentration of N species in soil	g mL^{-1}
[NH_3(g)]	concentration of gaseous NH_3 in soil air-filled pore space	g m^{-3}
[TAN(aq)]	concentration of aqueous TAN in soil water-filled pore space	g mL^{-1}
[TAN(s)]	concentration of exchangeable solid TAN adsorbed on soil particles	g m^{-3}
Δt	model time step	1 h
Δz_{soil}	transport distance in soils	m
$\Delta\theta$	incremental change in soil moisture	m^3 m^{-3} or m m^{-1}
$\sum_{\mathrm{NH_3}} v_i$	atomic diffusion volumes for NH_3	14.9
$\sum_{\mathrm{air}} v_i$	atomic diffusion volumes for air	20.1

References

Buss, S. R., Herbert, A. W., Morgan, P., Thornton, S. F., and Smith, J. W. N.: A review of ammonium attenuation in soil and groundwater, QJEGH, 37, 347–359, https://doi.org/10.1144/1470-9236/04-005, 2004.

Dardanelli, J. L., Ritchie, J. T., Calmon, M., Andriani, J. M., and Collino, D. J.: An empirical model for root water uptake, Field Crops Research, 87, 59–71, https://doi.org/10.1016/j.fcr.2003.09.008, 2004.

Dutta, B., Congreves, K. A., Smith, W. N., Grant, B. B., Rochette, P., Chantigny, M. H., and Desjardins, R. L.: Improving DNDC model to estimate ammonia loss from urea fertilizer application in temperate agroecosystems, Nutr Cycl Agroecosyst, 106, 275–292, https://doi.org/10.1007/s10705-016-9804-z, 2016.

Harmonized World Soil Database (version 1.2). https://daac.ornl.gov/SOILS/guides/HWSD.html#datacharact; last access: December 2022.

International Fertilizer Association (2021). https://www.fertilizer.org/ last access: November 2021.

Li, S., Zheng, X., Zhang, W., Han, S., Deng, J., Wang, K., Wang, R., Yao, Z., and Liu, C.: Modeling ammonia volatilization following the application of synthetic fertilizers to cultivated uplands with calcareous soils using an improved DNDC biogeochemistry model, Science of The Total Environment, 660, 931–946, https://doi.org/10.1016/j.scitotenv.2018.12.379, 2019.

Millington, R. J. and Quirk, J. P.: Permeability of porous solids, Trans. Faraday Soc., 57, 1200, https://doi.org/10.1039/tf9615701200, 1961.

Móring, A., Vieno, M., Doherty, R. M., Laubach, J., Taghizadeh-Toosi, A., and Sutton, M. A.: A process-based model for ammonia emission from urine patches, GAG (Generation of Ammonia from Grazing): description and sensitivity analysis, Biogeosciences, 13, 1837–1861, https://doi.org/10.5194/bg-13-1837-2016, 2016.

Parton, W. J., Mosier, A. R., Ojima, D. S., Valentine, D. W., Schimel, D. S., Weier, K., and Kulmala, A. E.: Generalized model for N_2 and N_2O production from nitrification and denitrification, Global Biogeochem. Cycles, 10, 401–412, https://doi.org/10.1029/96GB01455, 1996.

Parton, W. J., Holland, E. A., Del Grosso, S. J., Hartman, M. D., Martin, R. E., Mosier, A. R., Ojima, D. S., and Schimel, D. S.: Generalized model for NO_x and N_2O emissions from soils, J. Geophys. Res., 106, 17403–17419, https://doi.org/10.1029/2001JD900101, 2001.

Perry, R. H. and Green, D. W. (Eds.): Perry's chemical engineers' handbook, 8th ed., McGraw-Hill, New York, 1 pp., 2008.

Personne, E., Loubet, B., Herrmann, B., Mattsson, M., Schjoerring, J. K., Nemitz, E., Sutton, M. A., and Cellier, P.: SURFATM-NH3: a model combining the surface energy balance and bi-directional exchanges of ammonia applied at the field scale, 2009.

Riedo, M., Grub, A., Rosset, M., and Fuhrer, J.: A pasture simulation model for dry matter production, and fluxes of carbon, nitrogen, water and energy, Ecological Modelling, 105, 141–183, https://doi.org/10.1016/S0304-3800(97)00110-5, 1998.

Sherlock, R. and Goh, K.: Dynamics of ammonia volatilization from simulated urine patches and aqueous urea applied to pasture I. Field experiments, Fertilizer Research, 5, 181–195, https://doi.org/10.1007/BF01052715, 1984.

Stange, C. F. and Neue, H.-U.: Measuring and modelling seasonal variation of gross nitrification rates in response to long-term fertilisation, Biogeosciences, 6, 2181–2192, https://doi.org/10.5194/bg-6-2181-2009, 2009.

Sutton, M. A., Nemitz, E., Theobald, M. R., Milford, C., Dorsey, J. R., Gallagher, M. W., Hensen, A., Jongejan, P. A. C., Erisman, J. W., Mattsson, M., Schjoerring, J. K., Cellier, P., Loubet, B., Roche, R., Neftel, A., Hermann, B., Jones, S. K., Lehman, B. E., Horvath, L., Weidinger, T., Rajkai, K., Burkhardt, J., Lopmeier, F. J., and Daemmgen, U.: Dynamics of ammonia exchange with cut grassland: strategy and implementation of the GRAMINAE Integrated Experiment, 2009a.

Sutton, M. A., Nemitz, E., Milford, C., Campbell, C., Erisman, J. W., Hensen, A., Cellier, P., David, M., Loubet, B., Personne, E., Schjoerring, J. K., Mattsson, M., Dorsey, J. R., Gallagher, M. W., Horvath, L., Weidinger, T., Meszaros, R., Dammgen, U., Neftel, A., Herrmann, B., Lehman, B. E., Flechard, C., and Burkhardt, J.: Dynamics of ammonia exchange with cut grassland: synthesis of results and conclusions of the GRAMINAE Integrated Experiment, 2009b.

Thornley, J. H. M.: A Transport-resistance Model of Forest Growth and Partitioning, Annals of Botany, 68, 211–226, https://doi.org/10.1093/oxfordjournals.aob.a088246, 1991.

Thornley, J. H. M. and Cannell, M. G. R.: Nitrogen Relations in a Forest Plantation—Soil Organic Matter Ecosystem Model, Annals of Botany, 70, 137–151, https://doi.org/10.1093/oxfordjournals.aob.a088450, 1992.

Thornley, J. H. M. and Verberne, E. L. J.: A model of nitrogen flows in grassland, Plant Cell Environ, 12, 863–886, https://doi.org/10.1111/j.1365-3040.1989.tb01967.x, 1989.

Vira, J., Hess, P., Melkonian, J., and Wieder, W. R.: An improved mechanistic model for ammonia volatilization in Earth system models: Flow of Agricultural Nitrogen version 2 (FANv2), Geosci. Model Dev., 13, 4459–4490, https://doi.org/10.5194/gmd-13-4459-2020, 2020.

Wieder, W. R., Boehnert, J., and Bonan, G. B.: Evaluating soil biogeochemistry parameterizations in Earth system models with observations: Soil Biogeochemistry in ESMs, Global Biogeochem. Cycles, 28, 211–222, https://doi.org/10.1002/2013GB004665, 2014.